Progress In Electromagnetics Research C, Vol. 129, 273–287, 2023

Textile Dual Band Antenna Printed on Artificial Heart Bag for WBAN Communications

Walaa M. Hassan*

Abstract—This article presents a textile dual band antenna printed on an artificial heart (AH) bag for various Wireless Body Area Network (WBAN) communications. The textile dual band antenna operates at two different operating frequencies 2.4 GHz and 5 GHz. The two operating frequencies are reserved for IEEE 802.11b/g/n/ax and IEEE 802.11j WLAN standard. The designed antenna has a frequency bandwidth of (2.3642–2.5375 GHz) for the lower frequency of 2.4 GHz and (4.598–5.1683 GHz) for the upper frequency of 5 GHz. The dual band antenna is integrated with the proposed AH bag that is made from textile material. The effects of both different materials and dimensions of the proposed AH bag in the characteristics of the proposed antenna are investigated. The effect of the human body on the electrical performance of the proposed antenna integrated with the AH bag is presented. The amount of electromagnetic absorbed energy through the human body is also determined in terms of the specific absorption rate (SAR). The obtained SAR value is less than 0.12 W/Kg. This value meets the IEEE standards. Experimental verification for antenna integrated with AH bag and human body is presented.

1. INTRODUCTION

Recently, heart diseases have been a predominant cause of death. The numerical values of 23 million patients around the world who suffer from heart disease [1] are shown. Heart disease is expected to rise steadily in Japan as the population grows, reaching 1.3 million people by 2030. In 2006, 5.8 million persons in the United States had heart failure (HF), with 0.2 million having end-stage HF. In Russia, mortality from cardiovascular diseases is more than 50% of the total mortality. Artificial hearts (AH) are necessary to keep patients alive while they wait for a heart transplant, or if they are not eligible for a heart transplant [2]. Transplantation of donor and implantation of AH have been the best therapy of choice for many HF patients. Due to the scarcity of natural hearts, the "gold standard" is a donor heart transplantation [3]. Artificial hearts should have low profile, high reliability, low power density, and light weight [3, 4]. "Wearing Your Heart on Your Back" is the most interesting announcement for a portable AH device which provides the patients freedom whilst they wait for a donor and transplant. This wearable system is referred as Freedom portable driver [5–7]. It serves a greater essential purpose of circulating the blood of heart failure patients until a transplant becomes available. AH system is a 13.5 pound pack that connects with the aid of two tubes. Examples of actual portable AH devices are shown in Fig. 1.

Wireless Body Area Network (WBAN) has acquired a vital interest due to its many uses in health care, sports, battlefield, emergency operations, and care of the aged and underprivileged youngsters [8–10]. In WBAN, the presence of the human body poses an enormous challenge to the wearable antennas. By wearing these wearable devices, humans or animals can communicate directly. At the same time, they can communicate with other remote devices through wireless systems, which incorporate a sensor,

Received 9 January 2023, Accepted 7 February 2023, Scheduled 17 February 2023
* Corresponding author: Walaa Mohamed Hassan (walaa81hassan@yahoo.com).
The author is with the Electronics Research Institute (ERI), El-Nozha El-Gadida, Cairo 11843, Egypt.

Figure 1. Examples of portable AH devices.

microcontroller, and an antenna unit. The most demand for wireless communications technology with wide BW is achieved using miniaturized planar antennas to assist wireless devices, such as Industrial Scientific Medical (ISM) and Wireless Local Area Network (WLAN) [11–14]. Several factors should be considered in designing wearable antennas [15–20]. Several kinds of printed antennas can be used as wearable antennas [21–25]. The most widespread WLAN protocols are IEEE 802.11b/g, which utilizes the 2.4 GHz ISM band (2.4–2.485 GHz), and IEEE 802.11a, which employs the 5 GHz U-NII band and ISM band (5.15–5.825 GHz) [26, 27].

This paper presents a dual band antenna printed on the AH bag for different WBAN communications. The remaining parts of the paper are organized as follows. In Section 2, the proposed dual band antenna is designed on a textile material, and the electrical properties of the proposed antenna are studied In Section 3. Integration of the dual band antenna with the proposed AH bag made from textile jeans material is depicted. The effects of the change in the materials and dimensions of the AH bag on the electrical performance of the proposed antenna are studied in Section 3. The effect of the patient body on the electrical performance of the proposed antenna is studied in Section 4. In Section 5, the specific absorption rate (SAR) is calculated to show the effect of antenna radiation on the human body and to determine the amount of the electromagnetic energy absorbed inside the patient. Experimental verification of the designed dual band antenna integrated with a textile jeans bag and a human body is reported in Section 6.

2. DESIGN OF A DUAL BAND ANTENNA ON A TEXTILE SUBSTRATE

Textile antennas are quite suitable for wearable applications. A textile jeans substrate is used in the proposed antenna. This material has a suitable nature of the proposed AH bag. Textile jeans are the most wearable cloths because they are an ideal choice for all ages and more appropriate for the current lifestyle. Fig. 2 shows the geometry of the proposed dual band antenna. The dual band antenna consists of a radiating patch antenna mounted on a textile jeans fabric substrate with relative permittivity $\varepsilon_r = 1.6$ and dielectric loss tangent $\tan\delta = 0.02$ [21]. This patch antenna is fed by using a $50\,\Omega$ microstrip feed line. The radiator is a square patch with dimensions $L_P = W_p = 19.25$ mm. The thickness of the textile jeans fabric substrate is 1 mm. The dual band operation is acquired by means of using two rectangular slot rings which are etched on the ground as shown in Fig. 2. The dimensions of different parts of the proposed antenna are presented in Table 1.

Figure 3 shows the reflection coefficient of the designed antenna as a function of frequency. It can be seen that the antenna resonates at 2.4 GHz and 5 GHz with reflection coefficients less than -20 dB. The designed antenna has a frequency bandwidth of 173.3 MHz for the lower frequency of 2.4 GHz and 570.3 MHz for the upper frequency of 5 GHz. The two bands have sufficient bandwidth to cover the operating frequencies for IEEE 802.11b/g/n/ax applications and IEEE 802.11j WLAN applications [28, 29]. Two simulation software packages are used for the antenna design verification, High-Frequency Structure Simulator (HFSS) and CST [30, 31]. Good agreement between the two simulation techniques is shown in Fig. 3. Fig. 4 shows the current distributions for the proposed dual band antenna at three different frequencies within the operating band, 2.4 GHz, 4.9 GHz, and

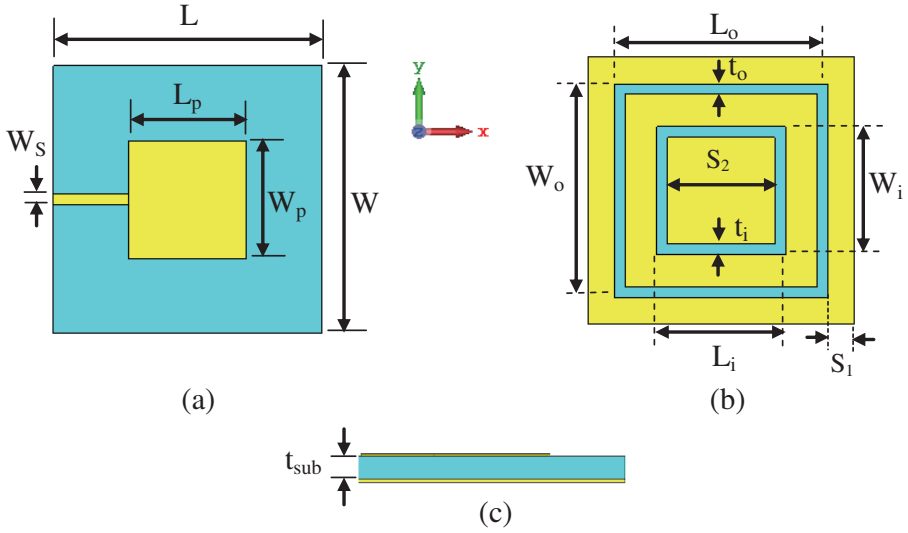

Figure 2. Geometry of the proposed antenna. (a) Front view. (b) Back view. (c) Side view.

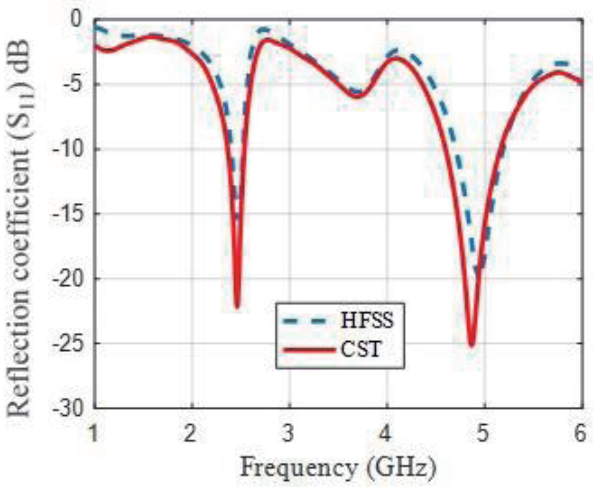

Figure 3. Reflection coefficient of the designed antenna.

Table 1. The dimensions of the proposed antenna.

Variable	Value (mm)	Variable	Value (mm)	Variable	Value (mm)
L	43.75	$\mathbf{L_o}$	35	$\mathbf{L_{bag}}$	200
W	43.75	$\mathbf{W_o}$	35	$\mathbf{W_{bag}}$	80
$\mathbf{L_P}$	19.25	$\mathbf{L_i}$	21	$\mathbf{H_{bag}}$	100
$\mathbf{W_P}$	19.25	$\mathbf{W_i}$	21	$\mathbf{T_{bag}}$	1.8
$\mathbf{W_S}$	1.75	$\mathbf{t_o}$	1.75	$\mathbf{S_1}$	4.375
$\mathbf{t_{sub}}$	1	$\mathbf{t_i}$	1.75	$\mathbf{S_2}$	17.5

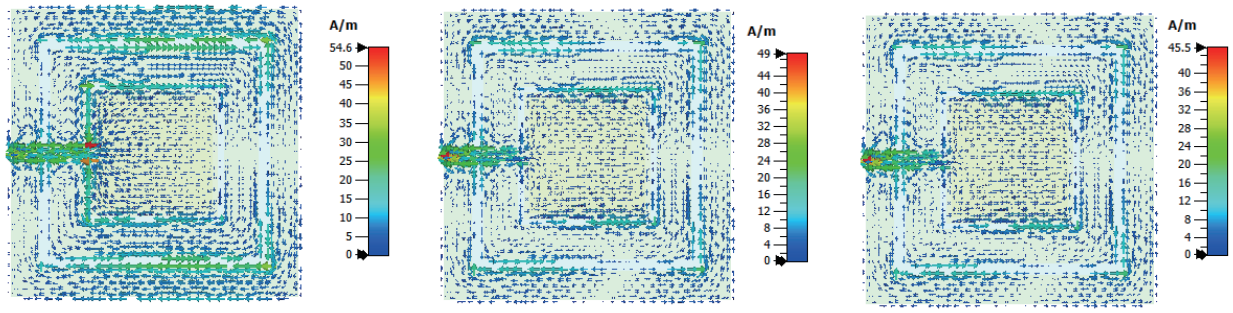

(a) (b) (c)

Figure 4. The current distributions along the proposed antenna at different operating frequencies (a) 2.4 GHz, (b) 4.9 GHz, (c) 5 GHz.

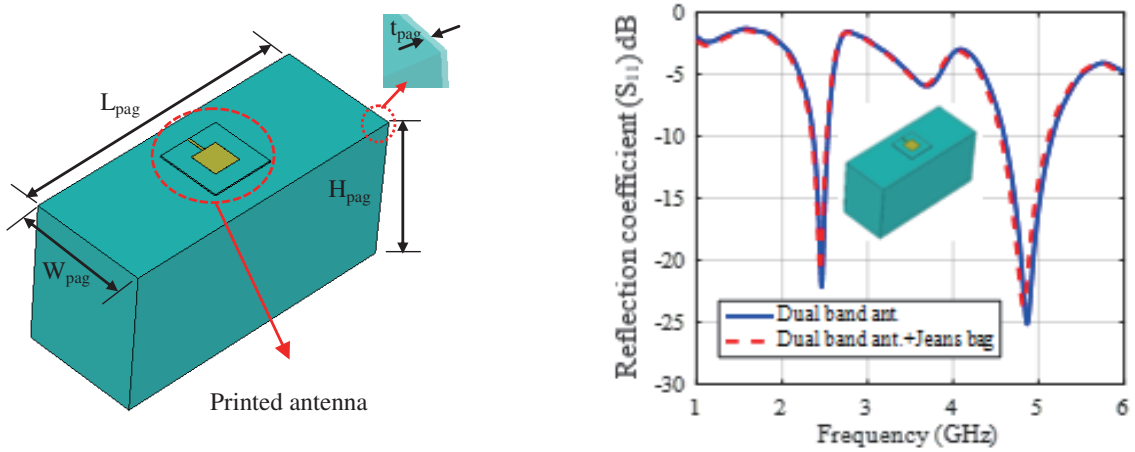

(a) (b)

Figure 5. (a) The geometry of the dual band antenna integrated with AH bag. (b) Reflection coefficient of the dual band antenna integrated with the textile jeans AH bag.

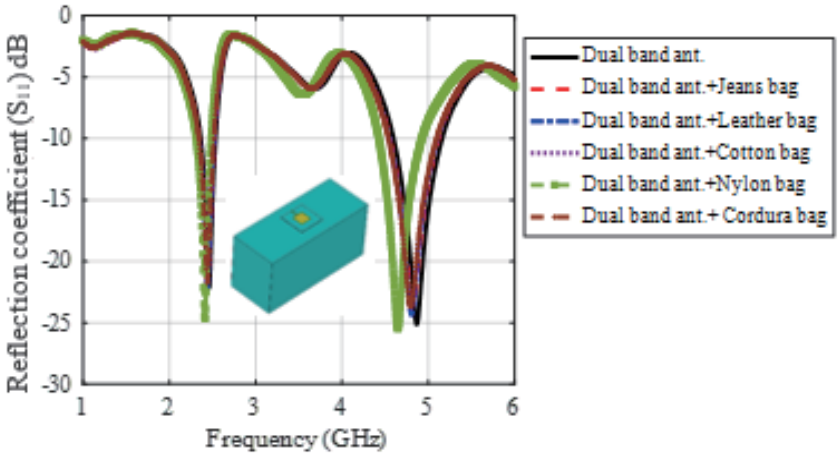

Figure 6. Reflection coefficient of the dual band antenna integrated with different materials of the AH bag.

5 GHz. The maximum gains at broadside direction are 2.39, 3.12, and 3.29 dBi for the three frequencies 2.4 GHz, 4.9 GHz, and 5 GHz, respectively.

3. DUAL BAND ANTENNA INTEGRATED WITH AH BAG

In this section, the dual band antenna is integrated with the proposed AH bag. The AH bag is made of jeans material. The antenna is integrated with the AH bag as shown in Fig. 5(a). The reflection coefficient of the proposed antenna integrated with the textile jeans AH bag is shown in Fig. 5(b). There is a slight difference between the proposed antenna in free space and the antenna integrated with the textile jeans AH bag. Different materials can also be used in this back bag as leather, cotton, nylon, or Cardura. The dielectric constants for leather, cotton, nylon, and Cardura are $\varepsilon_r = 1.8$ [32], $\varepsilon_r = 1.7$ $\varepsilon_r = 1.9$, and $\varepsilon_r = 1.4$, respectively. The corresponding loss tangents for these materials are: $\tan\delta = 0.02$, $\tan\delta = 0.025$ [33], $\delta = 0.0098$, and $\tan\delta = 0.0001$ [35], respectively. The effects of these different materials of the AH bag on the characteristics of the proposed antenna are negligible as shown in Fig. 6. The AH bag dimensions have significant effects on the performance of the designed antenna. Parametric study is presented for different sizes of the AH bag as shown in Fig. 7.

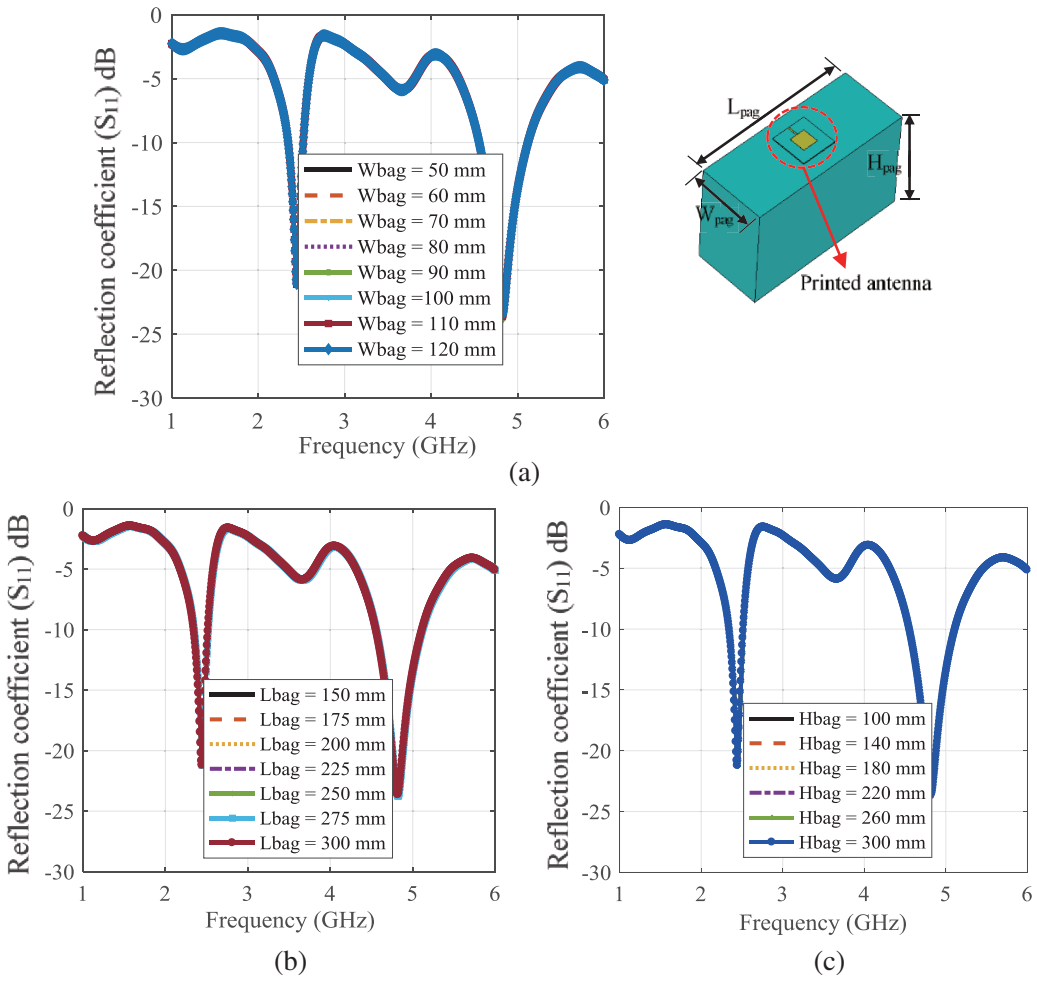

Figure 7. Reflection coefficient of the dual band antenna integrated with different sizes of the AH bag at (a) Different AH bag widths (Wbag). (b) Different AH bag lengths (Lbag), and (c) Different AH bag heights (Hbag).

4. THE EFFECT OF THE DUAL BAND ANTENNA ON THE PATIENT BODY

When the patient wears the AH bag, the wearable antenna is in proximity of the human body which is a lossy dielectric. The electromagnetic waves which are absorbed inside patient's body can have adverse health effects if the exposure limits are not observed [36]. It is important to study the amount of radiation inside the human body. The power density distribution inside the human body after adding the dual band antenna integrated with the AH bag to the human body is shown in Fig. 8. The specific absorption rate (SAR) levels are numerically investigated using the hugo voxel model in CST simulator [31] a body safety level. The reference power of 0.5 W is excited for the simulation in the SAR study. The most frequently used SAR limits are those of IEEE [37] which is 1.6 W/kg for any 1 g of tissue and ICNIRP (International Commission on Non-Ionizing Radiation Protection [38]) which is 2 W/kg for any 10 g of tissue. Fig. 9 shows the calculated SAR distribution along the human body after adding the dual band antenna with the AH bag at different WLAN frequencies 2.4 GHz, 4.9 GHz, and 5 GHz. The obtained maximum SAR value for the dual band antenna integrated with the AH bag at 2.4 GHz is 0.12 W/Kg average over 10 g of tissue. For frequencies 4.9 GHz and 5 GHz, the maximum SAR values are the same value 0.106 W/Kg average over 10 g of tissue. It can be noted that the absorbed power in human body is less than 0.12 W/Kg average over 10 g of tissue for the three operating frequencies, whose values are much smaller than the allowable limits of SAR.

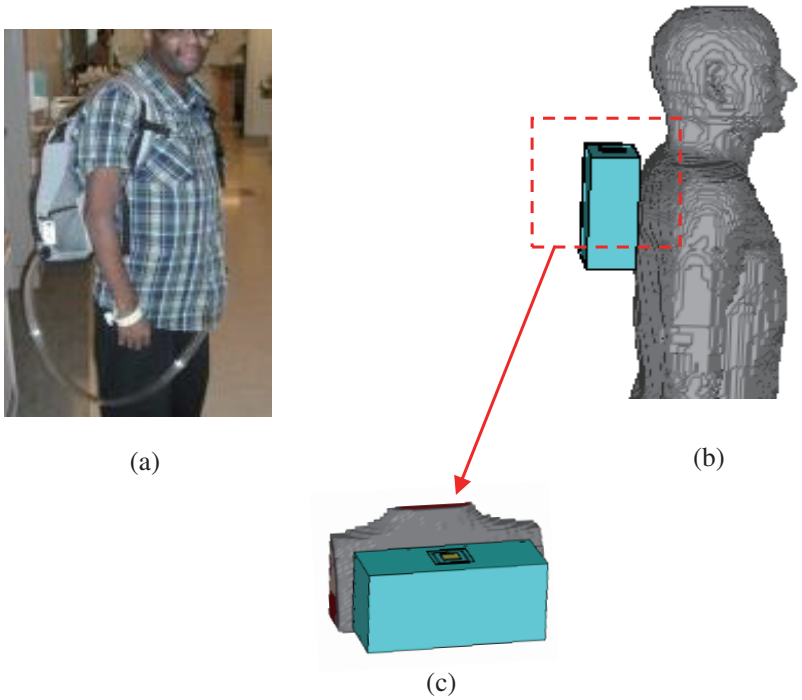

Figure 8. The AH bag antenna integrated with the human body. (a) Patient carrying an AH bag. (b) Simulation of AH bag on the back of the human body.

5. THE EFFECT OF THE PATIENT BODY ON THE DUAL BAND ANTENNA CHARACTERISTICS

The human body also has effects on the electromagnetics properties of the dual band antenna. The radiation efficiency and gain of the antenna are reduced due to the absorbed power by the human body. Fig. 10 shows the comparison of reflection coefficient of the dual band antenna integrated with textile jeans AH bag and human body with the reflection coefficients of both the proposed antenna and the proposed antenna integrated with the textile jeans AH bag on free space. In Fig. 10, it can be seen that

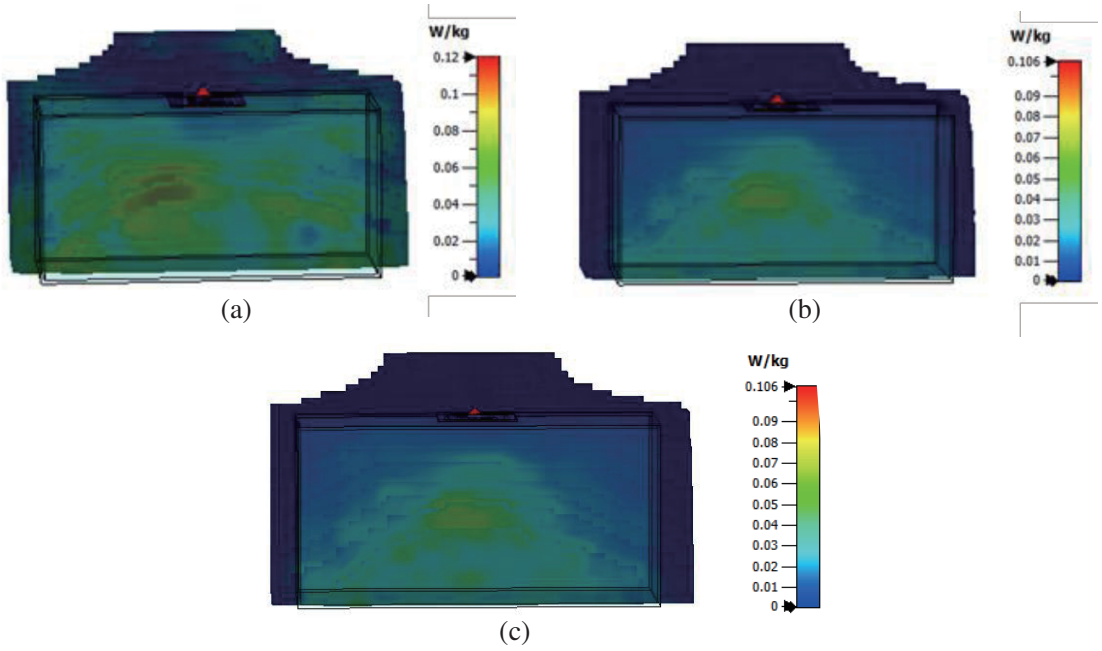

Figure 9. SAR simulation for the dual band antenna integrated withAH bag and integrated with the human body at different WLAN frequencies (a) $f = 2.4\,\text{GHz}$ (b) $f = 4.9\,\text{GHz}$ (c) $f = 5\,\text{GHz}$.

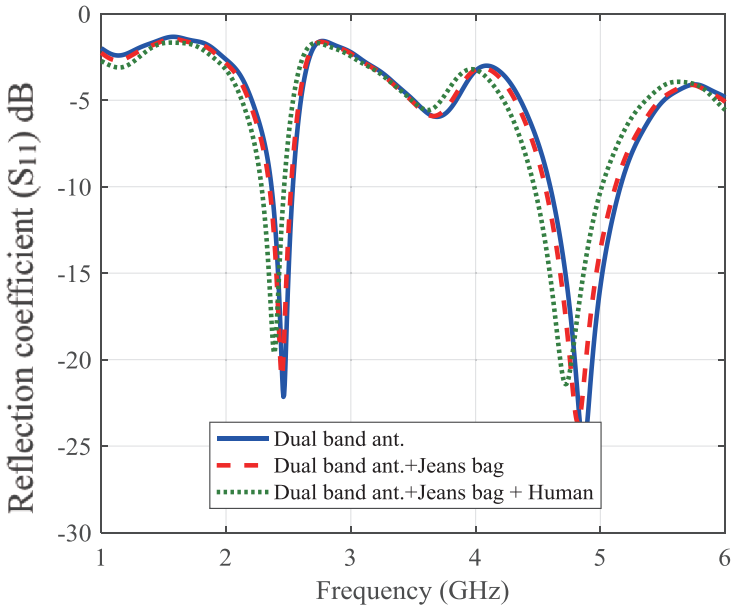

Figure 10. Reflection coefficient of the dual band antenna integrated with textile jeans AH bag and human body.

a little shift occurs in the resonance frequencies. The radiation patterns for the dual band antenna for the different cases including single antenna, antenna with textile jeans AH bag, and antenna with textile jeans AH bag on a human body are presented in Fig. 11. It can be noted that the maximum gains of the dual band antenna at 2.4 GHz, 4.9 GHz, and 5 GHz are 2.39 dBi, 3.12 dBi, and 3.29 dBi, respectively. The integration of the textile jeans AH bag and the human body with the dual band antenna has additional effects on the gain of the proposed antenna. The maximum gains for the dual band antenna

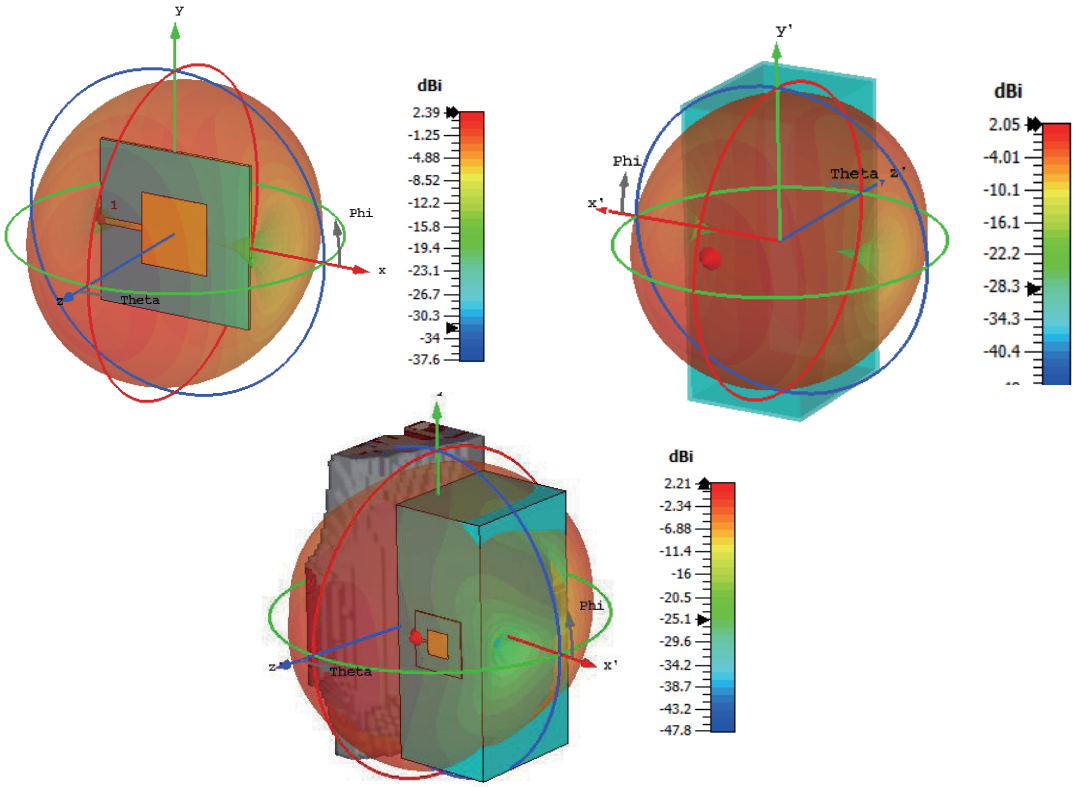

(a) $f = 2.4$ GHz

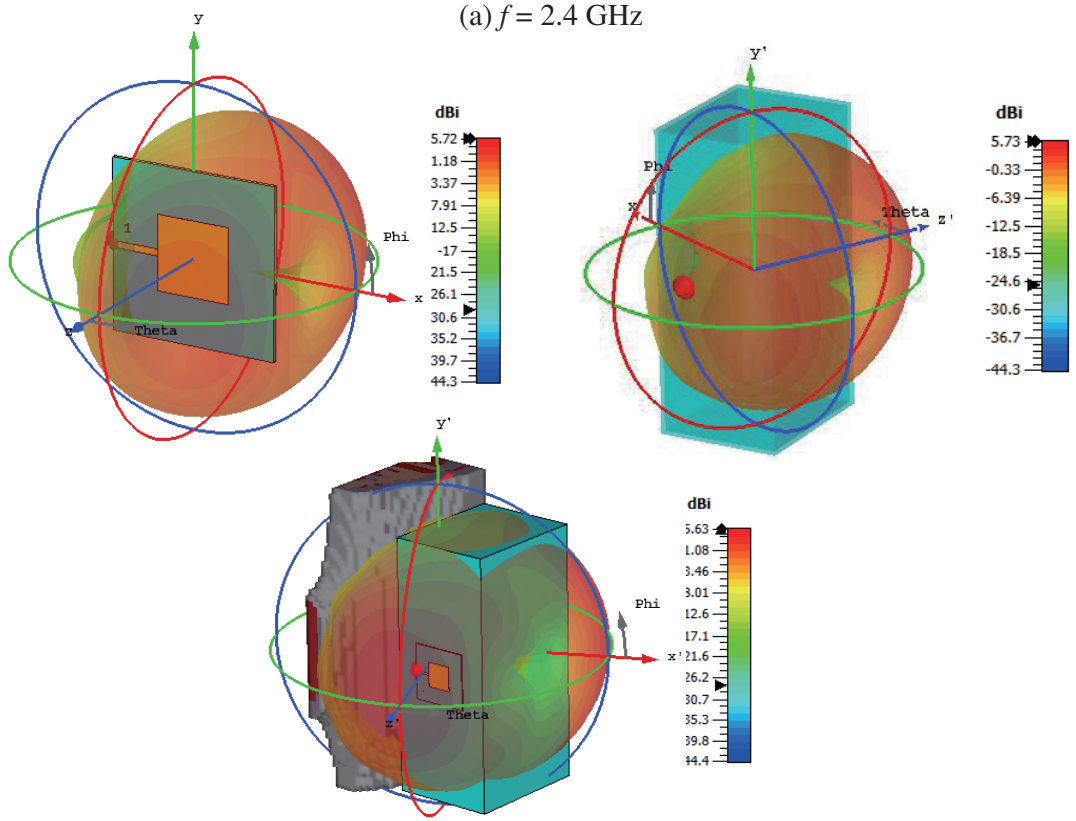

(b) $f = 4.9$ GHz

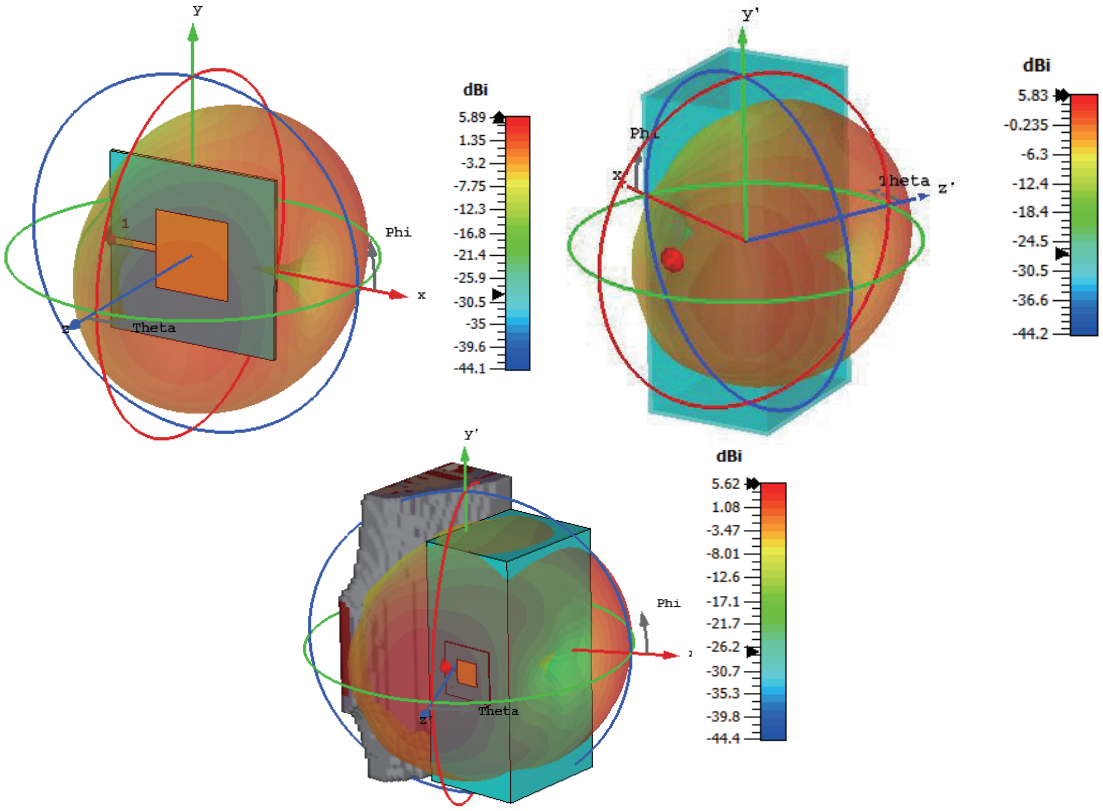

(c) $f = 5$ GHz

Figure 11. 3D radiation patterns for the dual band antenna, dual band antenna integrated with textile jeans AH bag, and dual band antenna with textile jeans AH bag and human body at different frequencies (a) $f = 2.4$ GHz. (b) $f = 4.9$ GHz. (c) $f = 5$ GHz.

integrated with AH bag at 2.4 GHz, 4.9 GHz, and 5 GHz are 2.05 dBi, 5.73 dBi, and 5.62 dBi, respectively. The corresponding maximum gains are 2.21 dB, 5.63 dB, and 5.83 dBi, respectively for the dual band antenna integration with the AH bag and human body. It can be noted that the gain is improved for the case of integrated antenna with the AH bag and mounted on the human body at the frequencies 4.9 GHz and 5 GHz.

6. EXPERIMENTAL VERIFICATION OF THE DESIGNED DUAL BAND ANTENNA INTEGRATED WITH TEXTILE JEANS AH BAG AND HUMAN BODY

Figure 12 shows the fabricated dual band antenna, dual band antenna integrated with the AH bag, and dual band antenna integrated with the AH bag and human body. Top and bottom views of the fabricated dual band antenna are shown in Figs. 12(a) and 12(b), respectively. The steps of building up the wearable antenna and integrating it with the AH bag are shown in Fig. 12. The wearable dual band antenna consists of three layers. The top layer is a square patch and microstrip line made of a copper sheet cut by a CNC machine. The top layer is fixed on the textile jeans fabric substrate material of thickness 1 mm by using adhesive double tape. This adhesive double tape has a negligible thickness compared with the textile jeans substrate. On the other side of the textile jeans substrate, there is a ground plane with two concentric square slots. The square slots on the ground plane are patterned also by using a CNC machine. The ground plane is fixed on the bottom side of the textile jeans substrate also by using adhesive double tape. The geometry of the proposed antenna is developed by using AutoCAD which is directly exported to the CNC machine. The dual band antenna is then fixed on the

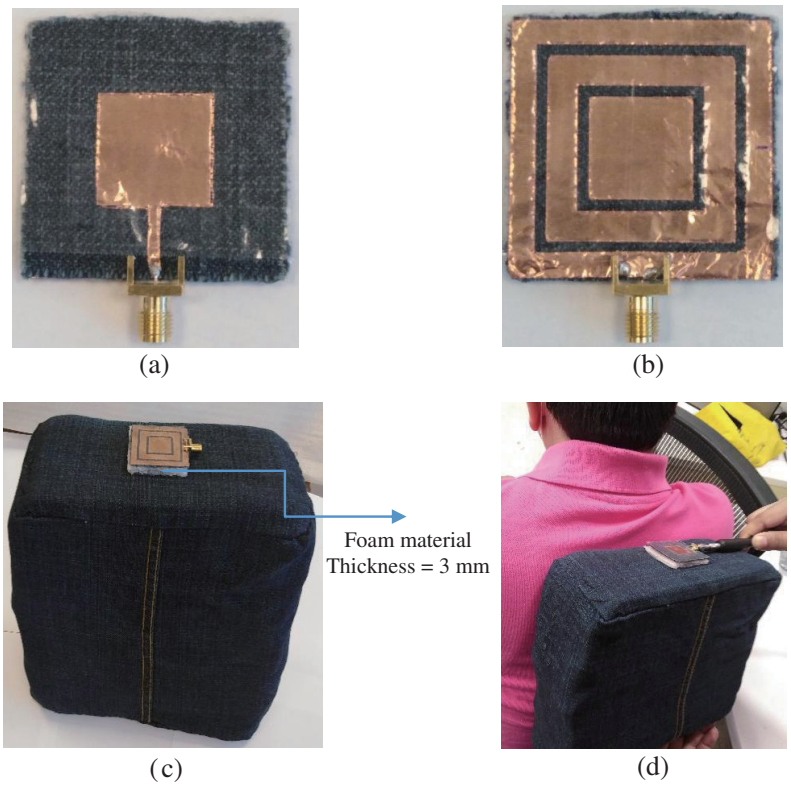

Figure 12. The fabrication and measurements steps. (a) Front view of the dual band antenna. (b) Bottom view of the dual band antenna. (c) Photographic of dual band antenna over the AH bag. (d) Photographic of dual band antenna over the AH bag and integrated with human. (a) Front view. (b) Bottom view. (c) Antenna + artificial heart bag. (d) Antenna + artificial heart bag + human.

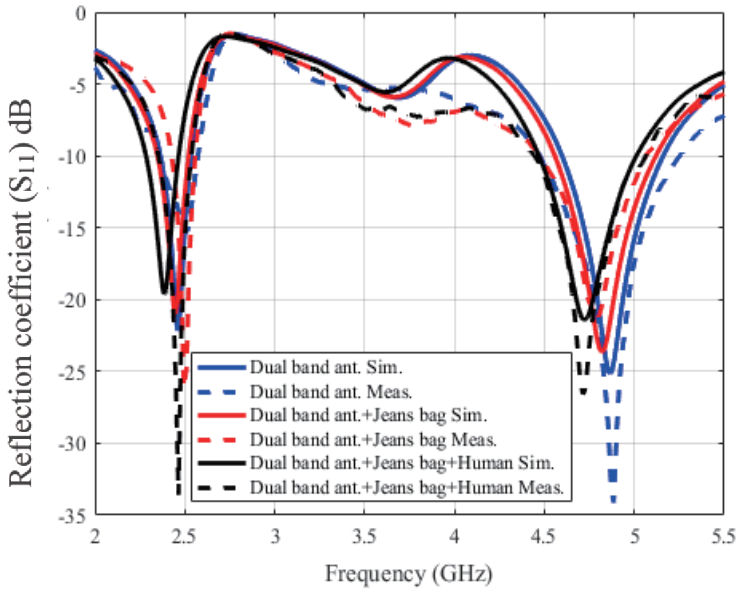

Figure 13. Comparison between measured and simulated of the return loss of the dual band antenna integrated with textile jeans AH bag, and dual band antenna with textile jeans AH bag and human body.

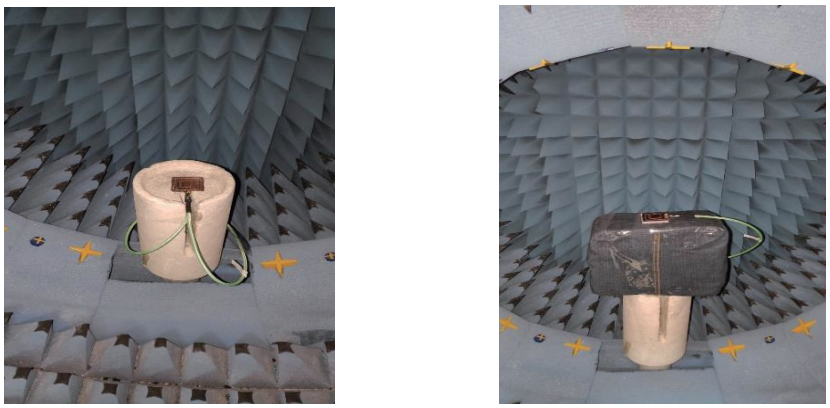

(a) (b)

Figure 14. Radiation pattern measurement setup of the fabricated antenna inside an anechoic chamber Inc. Model (NSI) 7005-30. (a) The dual band antenna. (b) The dual band antenna over the AH bag.

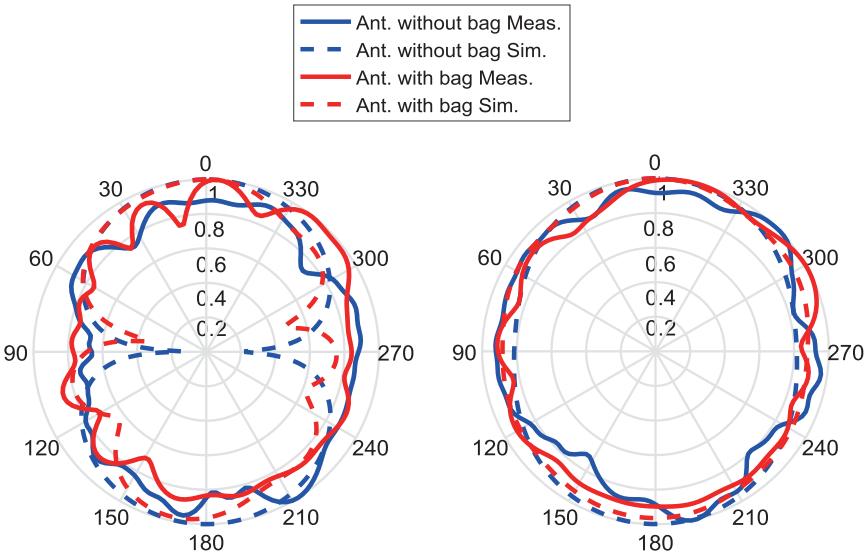

(a) (b)

Figure 15. Normalized measured and simulated radiation characteristic of the antenna with and without AH bag at $f = 2.4$ GHz for two planes (a) $phi = 0°$ (x-z plane) and (b) $phi = 90°$ (y-z plane).

AH bag using foam spacing with a width of 3 mm. The dual band antenna is fixed on the foam material and then on the AH bag by using adhesive double tape. The electrical properties of the fabricated wearable dual band antenna is measured by using a VNA Agilent N9918A. Comparison between the simulated and measured results is shown in Fig. 13. A good agreement between the simulated and measured results is achieved. It can be noted that the two operating bands shift slightly, but they still cover the two design bands, which fulfill the WLAN operating bands frequencies at 2.4 GHz and 5 GHz. The simulated and measured reflection coefficient magnitude S_{11} (dB) are below -10 dB for both operating bands frequencies at 2.4 GHz and 5 GHz. Radiation pattern measurement setup of the fabricated antenna inside an anechoic chamber Inc. Model (NSI) 7005-30 for the dual band antenna and the dual band antenna over the AH bag is shown in Fig. 14. Figs. 15, 16, and 17 show the normalized measured and simulated radiation characteristics of the antenna with and without AH bag at three

frequencies 2.4 GHz, 4.9 GHz, and 5 GHz, respectively. The radiation patterns are presented in x-z and y-z planes. It is apparent that the pattern is almost omnidirectional in the y-z plane, while in the x-z plane, the pattern is directional. It can be noted that the maximum measured gains of the dual band antenna with the AH bag and without the AH bag at the frequency of 2.4 GHz are 2.8 dB and 1.40 dB compared to the simulated values 2.39 dB and 2.05 dB, respectively. The measured gains are 5.52 dB and 3.48 dB compared to simulated gains 5.73 dB and 3.12 dB at the frequency of 4.9 GHz for the dual band antenna with AH bag and without AH bag. The measured gains at 5 GHz are almost the same as those at 4.9 GHz.

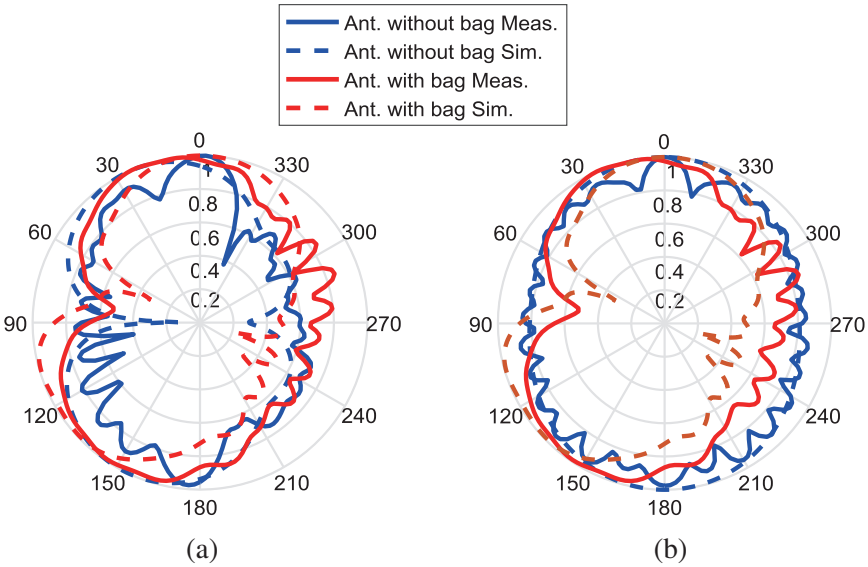

Figure 16. Normalized measured and simulated radiation characteristic of the antenna with and without AH bag at $f = 4.9$ GHz for two planes (a) $phi = 0°$ (x-z plane) and (b) $phi = 90°$ (y-z plane).

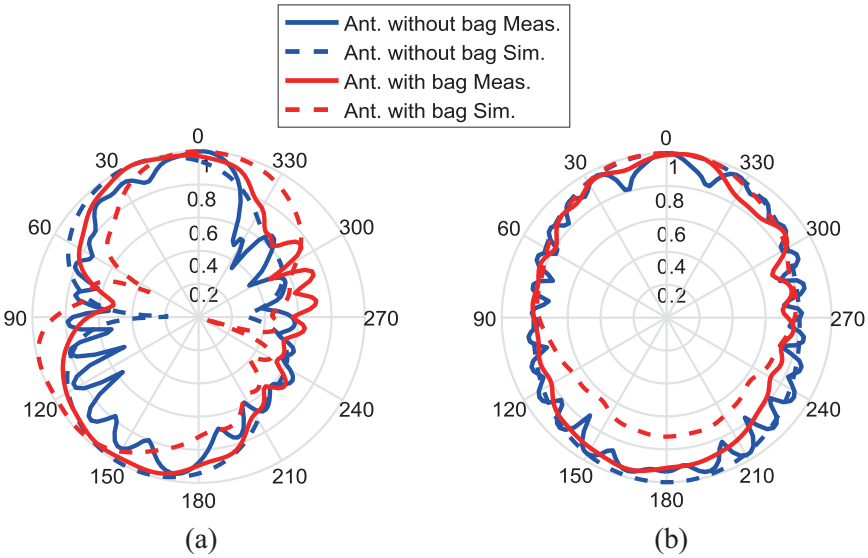

Figure 17. Normalized measured and simulated radiation characteristic of the antenna with and without AH bag at $f = 5$ GHz for two planes (a) $phi = 0°$ (x-z plane) and (b) $phi = 90°$ (y-z plane).

7. CONCLUSION

This paper presents the design of a compact dual band antenna integrated with an AH bag and a human body to cover the WBAN applications. The most widespread WLAN protocols are IEEE 802.11b/g, which utilizes the 2.4 GHz ISM band (2.4–2.485 GHz), and IEEE 802.11a, which employs the 5 GHz U-NII band and ISM band (5.15–5.825 GHz). Textile jeans are used as a substrate in the design of the proposed antenna. The designed dual band antenna operates at two center frequencies 2.4 GHz and 5 GHz. A good matching for the proposed antenna is achieved. Reflection coefficients for 2.4 GHz and 5 GHz are 22 dB and 26 dB, respectively. Good bandwidths are obtained at the two frequencies. The effects of integrating the proposed dual band antenna with the AH bag antenna are studied. It can be noted that there is only a slight variation between the antenna in free space and the antenna integrated with the textile jeans AH bag. The electromagnetic exposures into the human model from the proposed antenna integrated with AH bag at the three frequencies 2.4 GHz, 4.9 GHz, and 5 GHz are investigated and analyzed in terms of SAR. The SAR value of the antenna, when it is used with human body is less than 0.12 W/Kg average over 10 g of tissue for the two operating frequencies, and these values are less than the permissible limits. On the other hand, the effects of the human body on the proposed antenna performance are reported. The radiation efficiency and antenna gain are changed due to the absorbed power by the human body. This introduces a little shift in resonance frequencies. However, the antenna still operates in the required bands. Thus, the proposed antenna characteristics are suitable for a human body interface. Simulated results of the proposed antenna are tested and verified by the experimental ones. A good agreement between the simulated and measured results is obtained. The simulated and measured reflection coefficients are below −10 dB for both operating bands frequencies at 2.4 GHz and 5 GHz. The maximum measured gains of the proposed antenna for the lower cut-off frequency (2.4 GHz) and higher cut-off frequency (5 GHz) are 2.8 dB and 3.48 dB, respectively. With these remarkable features, the proposed antenna is useful for AH patients to be used in WBAN applications.

REFERENCES

1. Shcherbachev, A., I. Kudashov, S. Sergey, G.Itkin, A. Buchnev, E. Bychkov, and A. Galyamov, "Development of an artificial heart ventricles adaptive control system," *Symposium on Biomedical Engineering, Radioelectronics and Information Technology (USBEREIT)*, 78–81, April 2019.
2. Shiga, T., T. Kuroda, Y. Tsuboko, H. Miura, Y. Shiraishi, and T. Yambe, "Hemodynamic effects of pressure-volume relation in the atrial contraction model on the total artificial heart using centrifugal blood pumps," *35th Annual International Conference of the IEEE Engineering in Medicine and Biology Society (EMBC)*, 1815–1818, July 2013.
3. Ji, J., Z. Ling, J. Wang, W. Zhao, G. Liu, and T. Zeng, "Design and analysis of a Halbach magnetized magnetic screw for artificial heart," *IEEE Transactions on Magnetics*, Vol. 51, No. 11, 1–4, November 2015.
4. Shiba, K., M. Nukaya, T. Tsuji, and K. Koshiji, "Analysis of current density and specific absorption rate in biological tissue surrounding transcutaneous transformer for an artificial heart," *IEEE Transactions on Biomedical Engineering*, Vol. 55, No. 1, 205–213, January 2008.
5. Shah, R., Nilay, et al., "SynCardia portable freedom driver: a single-center experience with 11 patients," *Innovations*, Vol. 10, No. 3, 188–194, June 2015.
6. Mertz, L., "From artificial kidneys to artificial hearts and beyond: new developments offer great hope," *IEEE Pulse*, Vol. 3, No. 3, 14–20, May 2012.
7. Tang, Y. S., Y. C. Tsai, T. W. Chen, and S. Y. Li, "Artificial kidney engineering: the development of dialysis membranes for blood purification," *Membranes*, Vol. 12, No. 2, 177, 2022.
8. Abbasi, Q. H., M. Rehman, K. Qaraqe, and A. Alomainy, "Advances in body-centric wireless communication: applications and state-of-the-art," *Institution of Engineering and Technology*, 1–438, London, UK, 2016.

9. Seneviratne, S., Y. Hu, T. Nguyen, G. Lan, S. Khalifa, K. Thilakarathna, M. Hassan, and A. Seneviratne, "A survey of wearable devices and challenges," *IEEE Commun. Surv. Tutorials*, Vol. 19, 2573–2620, 2017.
10. Negra, R., I. Jemili, and A. Belghith, "Wireless body area networks: applications and technologies," *Procedia Comput. Sci.*, Vol. 83, 1274–1281, 2016.
11. Dakir, R., J. Zbitou, Mouhsen, A. Tribak, A. M. Sanchez, and M. Latrach, "A new compact and miniaturized multiband uniplanar CPW-fed monopole antenna with T-slot inverted for multiple wireless applications," *Int. J. Microw. Wirel. Technol.*, Vol. 9, 1541–1545, 2017.
12. Saraswat, R. K. and M. Kumar, "Design and implementation of a multiband metamaterial-loaded reconfigurable antenna for wireless applications," *International Journal of Antennas and Propagation*, 1–21, 2021
13. Ashyap, A. Y. I., Z. Z. Abidin, S. H. Dahlan, H. A. Majid, A. M. A. Waddah, et al., "Inverted E-Shaped Wearable Textile Antenna for Medical Applications," *IEEE Access*, Vol. 6, 35214–35222, 2018.
14. Paracha, K. N., A. D. Butt, G. Murtaza, S. A. Babale, and P. J. Soh, "Liquid metal antennas: materials, fabrication and applications," *Sensors*, Vol. 20, No. 1, 1–26, Otober 2020.
15. Nam, H. J., Y. S. Kim, Y. J. Kim, S. Y. Nam, and S. H. Choa, "Enhanced conductivity in highly stretchable silver and polymer nanocomposite conductors," *Journal of Nanoscience and Nanotechnology*, Vol. 21, No. 6, 3218–3226, 2021.
16. Kim, N., S. Lienemann, I. Petsagkourakis, et al., "Elastic conducting polymer composites in thermoelectric modules," *Nat. Commun.*, Vol. 11, No. 1, 1–10, 2020.
17. Dils, C., L. Werft, H. Walter, M. Zwanzig, M. Von Krshiwoblozki, and M. Schneider-Ramelow, "Investigation of the mechanical and electrical properties of elastic textile/polymer composites for stretchable electronics at quasi-static or cyclic mechanical loads," *Materials (Basel)*, Vol. 12, No. 21, November 2019.
18. Park, E. J., J. K. Sim, M.-G. Jeong, H. O. Seo, and Y. D. Kim, "Transparent and superhydrophobic films prepared with polydimethylsiloxane-coated silica nanoparticles," *RSC Adv.*, Vol. 3, No. 31, 12571–1257, 2013.
19. Janapala, D. K., M. Nesasudha, T. M. Neebha, and R. Kumar, "Design and development of flexible PDMS antenna for UWB-WBAN applications," *Wireless Personal Communications*, 1–17, 2022.
20. Liao, X., M. Dulle, J. M. D. S. E. Silva, R. B. A. Wehrspohn, et al., "High strength in combination with high toughness in robust and sustainable polymeric materials," *Science*, Vol. 366, 1376–1379, 2019.
21. Narmadha, R. G., M. Malathi, S. A. Kumar, T. Shanmuganantham, and S. Deivasigamani, "Performance of implantable antenna at ISM band characteristics for biomedical base," *ICT Express*, Vol. 8, No. 2, 198–201, 2022.
22. Vivek, N., S. Kumar, and K. Shambavi, "Design of wearable antennas for 5G applications," *Internatonal Journal of Electrical Engineering and Technology (IJEET)*, Vol. 12, 148–156, 2021.
23. Kaur, H. and P. Chawla, "Recent advances in wearable antennas: a survey," *The Industrial Internet of Things (IIoT) Intelligent Analytics for Predictive Maintenance*, 149–179, 2022.
24. Vidhya, S. S., K. G. Shanthi, P. Sivalakshmi, V. S. Reddy, V. L. Varma, V. D. Kumar, and Y. P. Reddy, "Design of UWB wearable microstrip patch antenna for wireless body worn applications," *AIP Conference Proceedings, AIP Publishing LLC*, Vol. 2523, No. 1, 020158, 2023.
25. Dhara, R., S. K. Jana, and M. Mitra, "Tri-band circularly polarized monopole antenna for wireless communication application," *Radioelectronics and Communications Systems*, Vol. 63, No. 4, 213–222, 2020.
26. Mazumdar, B., U. Chakraborty, and S. K. Chowdhury, "Design of compact printed antenna for WIMAX & WLAN applications," *Procedia Technology*, Vol. 4, 87–91, 2012.
27. Ashok Kumar, S. and T. Shanmuganantham, "Design and performance of textile antenna for wearable applications," *Transactions on Electrical and Electronic Materials*, 352–355, 2018.
28. 802.11 WiFi Standards Explained, *Lifewire*, Retrieved, 2018.

29. WiFi Frequency Bands List, www.radio-electronics.com, Retrieved 2018.
30. Ansoft High Frequency Structure Simulator (HFSS) ver. 14, Ansoft Corp., 2014.
31. CST Microwave Studio, ver. 2012, Computer Simulation Technology, Framingham, MA, 2012.
32. Regina, S. and A. Merline, "Flexible leather substrate dual-band wearable antenna with impact analysis on testing under wet condition for human rescue system," *Textile Research Journal*, 1–16, 2021.
33. Osman, M., M. Abd Rahim, N. Samsuri, H. Salim, and M. Ali, "Embroidered fully textile wearable antenna for medical monitoring applications," *Progress In Electromagnetics Research*, 321–337, 2011.
34. Engineering ToolBox, *Relative Permittivity — The Dielectric Constant*, 2010, [online] Available at: https://www.engineeringtoolbox.com/relative-permittivity-d_1660.html.
35. Peng, H., *Fiber Electonics*, Springer Nature Singapore Pte Ltd., 2020.
36. Kumar, S. A. and S. Thangavelu, "Design and analysis of implantable CPW fed X-monopole antenna for ISM band applications," *Telemed. e-Health*, Vol. 20, No. 3, 246–252, 246, 2014.
37. IEEE Standards for Safety Levels With Request to Human Exposure to Radiofrequency Electromagnetic Fields, 3 kHz to 300 GHz, IEEE Std. C95.1, 1999.
38. ICNIRP (International Commission on Non-Ionizing Radiation Protection), "Guidelines for limiting exposure to time-varying electric magnetic, and electromagnetic fields (up to 300 GHz)," *Health Phys.*, Vol. 74, 494–522, 1998.